PRINT ISSN 1119-8362
Electronic ISSN 2659-1499

Full-text Available Online at
https://www.ajol.info/index.php/jasem
https://www.bioline.org.br/ja

J. Appl. Sci. Environ. Manage.
Vol. 29 (3) 925-937 Mar. 2025

Potential Impacts of Future Variation in Temperature and Rainfall on Hydrology and Sediment Yield in a Water Catchment in Central Uganda

[1,3*]MWANGU, AR; [2]OINDO, BO; [3]MASIKA, DM

*[*1]Department of Geography, Kabale University, Uganda*
[2]Department of Environmental Sciences, Maseno University, Kenya
[3]Department of Geography and Natural Resources Management, Maseno University, Kenya

**Corresponding Author Email: amwangu@gmail.com*
**ORCID: https://orcid.org/0000-0002-1342-4772*
**Tel: +256 703 451945*

Co-Authors Email: bonifaceoindo@gmail.com; masikaden@gmail.com

ABSTRACT: Upper Ssezibwa catchment is experiencing variations in temperature and rainfall affecting the hydrological process through variable surface runoff, increased sediment yield, siltation of river channels leading to increased flooding in the lower part of the catchment. All of these degrade the environment and affect the sustainability of the water resources. Climate projections indicate a progressive increase in rainfall and temperatures in the catchment and requires attention. Hence, the objective of this paper was to evaluate the potential impacts of future variation in temperature and rainfall on hydrology and sediment yield in a water catchment in central Uganda using appropriate standard methods. Results for Soil and Water Assessment Tool (SWAT) model calibration- (R^2=0.85, NSE=0.82, KGE=0.76, PBIAS = -18.5) and validation (R^2=0.72, NSE=0.66, KGE=0.66, PBIAS= -19.3) indicate a good agreement with the observed values. The model projected 1.3^{0}C and 1.5^{0}C increase in temperature and 10.9% and 10.4% relative change in precipitation for the period 2025-2055 under RCP 4.5 and RCP 8.5 emission scenarios. Future projections show climate variability will lead to increase in surface runoff and sediment yield during rainfall peaks is likely to increase river discharge, silting of the river channel and flood occurrence. Quantifying water balance and sediment yield within the catchment is crucial for planning downstream projects and water management generally.

DOI: https://dx.doi.org/10.4314/jasem.v29i3.31

Cite this Article as: MWANGU, A. R; OINDO, B. O; MASIKA, D. M (2025) Potential Impacts of Future Variation in Temperature and Rainfall on Hydrology and Sediment Yield in a Water Catchment in Central Uganda. *J. Appl. Sci. Environ. Manage.* 29 (3) 925-937

Dates: Received: 30 January 2025; Revised: 12 March 2025; Accepted: 19 March 2025; Published: 31 March 2025

Keywords; climate variability; temperature; rainfall; hydrology; sediment yield

Climate variability is emerging as a key factor in the modification of hydrology and sediment yield globally. The progressive global warming and climate variation has altered the hydrological processes worldwide in different directions and degrees (Thackeray *et al.,* 2022; Dou *et al.,* 2022). Perron (2017) observes that climate has a significant moderating effect on mass-wasting and erosion processes, determining sediment yield at both the geological and event time scales, and shaping basins and river networks. In hill slopes and water catchments, the production and transfer of sediments are governed by probable changes in air temperature, precipitation and runoff (Hirschberg *et al.,* 2020). In recent years, climate variability greatly influenced the hydrological processes in water catchments (Dai *et al.,* 2020; dos Santos *et al.,* 2021). Sok *et al.,* (2022) Tamm *et al.,* (2018) note that climate variability influences hydrology by modifying the flow regimes of rivers and altering the water availability. Further,

**Corresponding Author Email: amwangu@gmail.com*
**ORCID: https://orcid.org/0000-0002-1342-4772*
**Tel: +256 703 451945*

Choudhury *et al.* (2019) observed that changes in rainfall amount and temperature are responsible for various environmental challenges including floods and channel sedimentation. On the other hand, Kandissouron *et al.,* (2018) noted that high temperatures and the drought of the early 1970s in West Africa caused devastating consequences on lakes, rivers and wetlands which are principal water resources affecting the local people's water needs and livelihoods. Recent studies have established that change in global climate, specifically the observed increase in Land Surface Temperature (LST) has affected water resources as well as vegetated areas (Abd El-Hamid *et al.,* 2020). Climatic factors affect the environment through increased soil erosion and floods through heavy rainfall (Ochola *et al.,* 2019) while changes in temperature leads to droughts that have resulted into forest loss through forest fires as well as deforestation which affect stream discharge (Almagro *et al.,* 2020). Additionally, changes in climate parameters cause a shift in water availability and LULC change at the watershed scale (Beharry *et al.,* 2021).

Numerous studies have examined the effect of climate variability on river discharge regimes and sediment yield in various locations. Lu *et al.,* (2013) revealed that climate variability represented by raising temperatures affect precipitation regimes, surface hydrology and sediment delivery dynamics. In fact, Lu *et al.,* (2013) observed that rising temperatures coupled with lower precipitation substantially reduced sediment loads delivered into the sea by 4 - 61%. Azari *et al.,* (2016) observed that the changing climate expedite the hydrological cycle, modifying the rainfall as well as magnitude and timing of runoff noting an increase in river discharge of 5.8%, 2.8% and 9.8%; and an increase in sediment yield of 47.7%, 44.5% and 35.9% respectively inferring that the effect of rainfall and temperature variations is greater on sediment yield than river discharge. Further, Azari *et al.,* (2016) noted that the decrease of sediment yield and river discharge is more striking in summer (July – September) while the increase is more prominent in wet season. Upper Ssezibwa catchment has a complex ecosystem characterized by seasonal flooding with noticeable bearings on water resources and sediment yield in the catchment but has not gotten scientific attention.

Changes in river flow behavior is a challenge to people in Upper Ssezibwa catchment and their livelihoods. Whenever the basin experiences floods, people are seriously affected indicating that the planners may not be aware of the forcings of the changes, therefore choosing appropriate land and water management practices and devising strategies for sustainable management of natural resources in the basin is difficult. Simulating hydrological responses to LULC change and climate variability is important for decision-makers in improving human wellbeing (Engida *et al.,* 2021). In fact, Getahun and Van Lanen (2015) observed that catchment studies could provide straight evidence of LULC change and climate on hydrology. For this reason, Karvonen *et al.,* (1999); Bhatta *et al.,* (2019); Banda (2022) note that hydrological models have increasingly become crucial for researching the effects of climate variability on the hydrological cycle in a landscape. Studies simulating future impacts of LULC change and climate variability on hydrology and sediment yield are emerging in sub-Saharan Africa but still in their infancy. Variations in temperature and rainfall has been observed in Upper Ssezibwa catchment. Rainfall peaks led to flooding of River Ssezibwa and subsequently displacement of people, destruction of infrastructure and property as well as loss of lives (Ampurire, 2018; Muzaale, 2007; 2019; Kimbowa, 2019; The *Independent*, 2020 June 22; Nasasira, 2021).

There is scarcity of studies assessing the influence of climate variability on hydrology and sediment yield in Upper Ssezibwa catchment. Hence, the objective of this paper was to evaluate the Potential impacts of future variation in temperature and rainfall on hydrology and sediment yield in a water catchment in central Uganda

MATERIALS AND METHODS

Study area: The upper Ssezibwa catchment spans 254.08 km^2 in Central Uganda between 00°16′12″N, 33°00′18″E, and 01°24′00″N: 32°44′06″E (Figure 1). The ecosystem products and services that sustain human life make the Upper Ssezibwa watershed a valuable ecosystem zone. Upper catchment of Ssezibwa has fertile clay loam soils and a tropical climate with a bimodal rainfall distribution that includes two wet seasons—March to May for long rains and September to November for short rains draw smallholder farmers who remove vegetation cover and carry out their agricultural activities. Temperature and precipitation variations are the main causes of the River Ssezibwa's fluctuations. The catchment sees high flows during the rainy seasons, which lead to floods, and low flows during the dry seasons which cause droughts and water scarcity. Floods and soil erosion cause sediment loading in the Upper Ssezibwa catchment (NEMA, 2014).

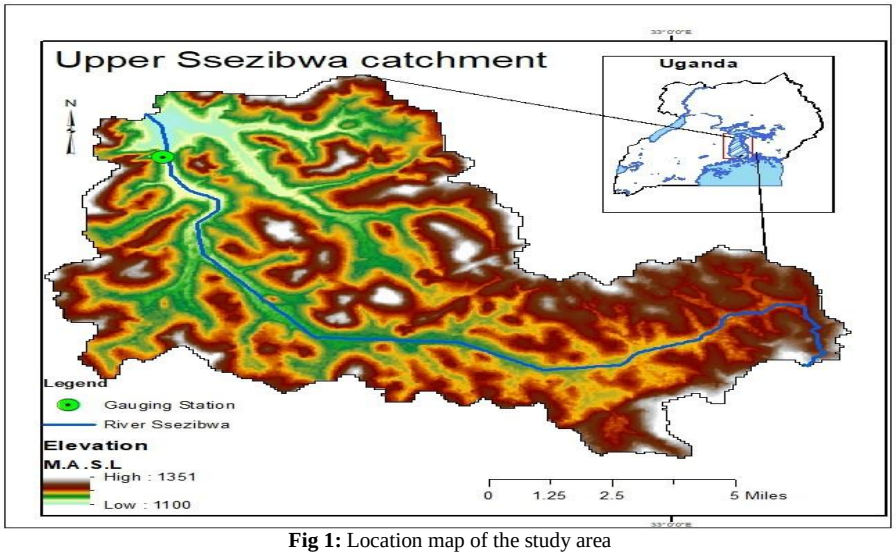

Fig 1: Location map of the study area

Input data: The SWAT hydrological modelling at the catchment level require temporal and spatial data. Temporal data include hydrological, sediment and climatic data, which are used to setup the model and hydrological processes, and spatial data in particular the soil map, the land use land cover map and the digital elevation model (DEM). The United States Geological Survey (USGS) provided the DEM with a 30-m resolution which was used to extract spatial extent of the catchment, extract the topographic parameters such as the steepness and length of the slope and generate properties of the stream network that are required for the SWAT model. The USGS provided a LULC map of the catchment in a resolution of 30 m that contained seven LULC classes, namely built- up areas, small scale farming, commercial farming, grassland, wetland, shrubland and woodland. The physical and chemical properties of the study basin were taken from the database of The World Food and Agriculture Organization of the United Nations (FAO) FAO/UNESCO soil map of the world. The National Aeronautics and Space Administration (NASA) portal for forecasting global energy resources (*https://power.larc.nasa.gov/*) provided meteorological data for the Upper Ssezibwa catchment, including daily minimum and maximum temperatures, precipitation, solar radiation, wind speed, and relative humidity. Hydrological data was accessed from the Ministry of Water and Environment while sediment data was computed from the samples collected from the catchment. Historical time series (1980–2010) daily agro-meteorological data specifically daily temperature (maximum and minimum) and daily precipitation, wind speed (maximum), solar radiation and relative humidity (maximum and minimum) which are required for climate projection was downloaded from the NASA portal for prediction of worldwide energy resources (*https://power.larc.nasa.gov/*). This data is recommended for use in areas with non-functional weather stations. The baseline period of 1980-2010 was used to project the future climate in the study area. The projection of future climate was done using the Agricultural Model Intercomparison and Improvement Project (AgMIP) as well as R software. The projection utilized the delta method, which is based on the sum of interpolated anomalies to high-resolution monthly climate surfaces. The method produces a smoothed (interpolated) surface of changes in climates (deltas or anomalies) and then applies this interpolated surface to the baseline climate, taking into account the possible bias due to the difference in baselines (Navarro-Racines et al., 2020). Twenty-nine (29) general circulation models (GCM) embedded in AgMIP protocol were used (Table 1). The 29 GCMs were used for intercomparison of the ensemble data from various models/scenarios taking note of the anomalies of some GCM arising from differences in formulation among numerical models, differences in emission scenarios, and the natural variability of the climate system against the observed data of the catchment. The use of these GCMs helped to downscale the climate data and eliminating discrepancies of outputs from the projections at the global level which would not well reflect evidence on a small local area thus generating more consistent and transferable findings based on common simulation protocols. The projection was done up to 2055 under two Representative Concentration Pathways (RCP4.5 and RCP8.5).

.

Table 1. Summary of 29 GCMs that form the ensemble of climate projections used in the study

GCM	Institution	Horizontal resolution	2x [CO2] Eq. climate Sens. (°C)
ACCESS1-0	Commonwealth Scientific and Industrial Research Organization (CSIRO) and Bureau of Meteorology (BOM), Australia	1.25° × 1.875°	3.8
BCC-CSM1-1	Beijing Climate Center, China Meteorological Administration	~2.8° × 2.8°	2.8
BNU-ESM	College of Global Change and Earth Systems Science, Beijing Normal University (BNU)	~2.8° × 2.8°	4.1
CanESM2	Canadian Centre for Climate Modelling & Analysis	~2.8° × 2.8°	3.7
CCSM4	US National Center for Atmospheric Research (NCAR)	~0.9° × 1.25°	2.9
CESM1-BGC	US National Science Foundation (NSF), US Department of Energy (DOE), and the US National Centre for Atmospheric Research (NCAR)	~0.9° × 1.25°	n.a.
CMCC-CM	Euro-Mediterranean Center on Climate Change	~0.75° × 0.75°	n.a
CMCC-CMS	Euro-Mediterranean Center on Climate Change	~1.9° × 1.875°	n.a.
CNRM-CM5	France National Centre for Meteorological Research	~1.4° × 1.4°	3.3
CSIRO-Mk3-6-0	Queensland Climate Change Centre of Excellence and Commonwealth Scientific and Industrial Research Organization (CSIRO)	~1.9° × 1.875°	4.1
FGOALS-g2	Chinese Academy of Sciences	~2.8° × 2.8°	n.a.
GFDL-CM3	NOAA/Geophysical Fluid Dynamic Laboratory (GFDL)	2.0° × 2.5°	4
GFDL-ESM2G	NOAA/Geophysical Fluid Dynamic Laboratory (GFDL)	~2.0° × 2.5°	2.4
GFDL-ESM2M	NOAA/Geophysical Fluid Dynamic Laboratory (GFDL)	~2.0° × 2.5°	2.4
GISS-E2-H	National Aeronautics and Space Association Goddard Institute for Space Studies (NASA GISS)	2° × 2.5°	2.3
GISS-E2-R	National Aeronautics and Space Association Goddard Institute for Space Studies (NASA GISS)	2° × 2.5°	2.1
HadGEM2-AO	UK Meteorological Office - Hadley Centre	1.25° × 1.875°	n.a.
HadGEM2-CC	UK Meteorological Office - Hadley Centre	1.25° × 1.875°	n.a.
HadGEM2-ES	UK Meteorological Office - Hadley Centre	1.25° × 1.875°	4.6
INMCM4.0	Russian Institute for Numerical Mathematics (INM)	1.5° × 2°	2.1
IPSL-CM5A-LR	Institute Pierre Simon Laplace (IPSL)	~1.9° × 3.75°	4.1
IPSL-CM5A-MR	Institute Pierre Simon Laplace (IPSL)	~1.3° × 2.5°	n.a.
IPSL-CM5B-LR	Institute Pierre Simon Laplace (IPSL)	~1.9° × 3.75°	2.6
MIROC5	University of Tokyo, Japanese National Institute for Environmental Studies (NIES), and Japan Agency for Marine-Earth Science and Technology (JAMSTEC)	~1.4° × ~1.4°	2.7
MIROC-ESM	University of Tokyo, Japanese National Institute for Environmental Studies (NIES), and Japan Agency for Marine-Earth Science and Technology (JAMSTEC)	~2.8° × ~2.8°	4.7
MPI-ESM-LR	Max Planck Institute (MPI) for Meteorology (low resolution)	~1.9° × 1.875°	3.6
MPI-ESM-MR	Max Planck Institute (MPI) for Meteorology (mixed resolution)	~1.9° × 1.875°	n.a
MRI-CGCM3	Japanese Meteorological Research Institute (MRI)	~1.1° × 1.125°	2.6
NorESM1-M	Norwegian Climate Centre	~1.9° × 2.5°	2.8

SWAT model setup: The SWAT model is an eco-hydrological, physical and semi-distributed model that works in a daily time step and has been extensively used in environmental and hydrological studies, owing to its capability to simulate diverse hydrological processes (Arnold *et al*., 1998). The major components of the SWAT include, soil temperature and properties, stream routing and pond/reservoir routing weather, hydrology, land management, erosion/sedimentation, nutrients, pesticides and plant growth. The SWAT simulates the land phase of the hydrologic model based on water balance equation (1);

$$SW_t = SW_o + \Sigma_{i=1}^{t} = \left(R_{day} - Q_{surf} - E_a - W_{seep} - Q_{gw}\right) \quad (1)$$

Where; SW_t = Final soil water content (mm), SW_o = Initial soil water content (mm), t = Time (days), R_{day} = Amount of precipitation on day i (mm), Q_{surf} = quantity of surface runoff (mm), E_a = Evapotranspiration (mm), W_{seep} = Seepage from the bottom soil layer (mm), and Q_{gw} = Ground water flow (mm).

The Modified Universal Soil Loss Equation (MUSLE) embedded in SWAT was used for sediment flow analysis. The MUSLE equation used to calculate the sediment from the catchment is;

$$S = 11.8(Q \times Area \times pr)^{0.56} \times K \times C \times P \times LS \times R \quad (2)$$

Where, S = Sediment load (mt), Q = Surface runoff (cu. m), pr = Peak runoff rate (cu. m), K = USLE soil erodibility factor, C = Cover and management factor, P = support practice factor, LS = Topographic factor (gradient, length).

Sensitivity analysis: The calibration, validation and sensitivity analysis of the model was done using Semi-automatic Sequential Uncertainty Fitting 2 (SUFI-2) in SWAT Calibration and Uncertainty Procedures (SWATCUP) optimization programme. The Global Sensitivity Analysis (GSA) was used in sensitivity analysis because it allows investigating the whole assortment of parameters. Under this method, the entire parameters under consideration were concurrently perturbed permitting investigation of parameter connections and their impacts on model outputs (Abbaspour, 2015; Cibin *et al.,* 2010).

Model performance evaluation: Four major criteria were used to assess the evaluation of performance as suggested by (Moriasi *et al.,* 2007; Gupta *et al.,* 2009) namely; Nash–Sutcliffe efficiency (NSE), Coefficient of determination (R^2), Percent Bias (PBIAS) and the Kling–Gupta efficiency (KGE).

Nash–Sutcliffe efficiency (NSE): Indicates the goodness of fit of the plot between the measures and simulated datasets

$$NSE = 1 - \left[\frac{\sum_{i=1}^{n}(Y_i^{obs} - Y_i^{sim})^2}{\sum_{i=1}^{n}(Y_i^{obs} - Y^{mean})^2}\right] \quad (3)$$

where *Yi obs* is the *i*th observation for the constituent being evaluated, *Yi sim* is the *i*th simulated value for the constituent being evaluated, *Ymean* is the mean of observed data for the constituent being evaluated, and n is the total number of observations (Moriasi *et al.,* 2007)

Kling–Gupta efficiency (KGE): It is a metric for evaluating the goodness-of-fit of the model simulations and corresponding observations. Besides measuring the accuracy of the model predictions, it also measures the model's ability to reproduce the variability and timing of the observed data.

$$KGE = 1 - \sqrt{(r-1)^2 + (\alpha - 1)^2} + (\beta - 1)^2 \quad (4)$$

r is the Pearson correlation coefficient, α is a term representing the variability of prediction errors, β is a bias term. The term α and β are defined as follows $\beta = \frac{\mu_s}{\mu_0}$ Where; μ_s is the mean of the simulated time series (e.g.: flows predicted by the model) and μ_0 is the mean of the observed time series (Moriasi *et al.,* 2007)

Percent bias (PBIAS): Measures the tendency for observed to be greater (or lesser) than the simulated

$$PBIAS = \left[\frac{\sum_{i=1}^{n}\left((Y_i^{obs} - Y_i^{sim})\right) * 1(100)}{\sum_{i=1}^{n}(Y_i^{obs})}\right] \quad (5)$$

Where: Y^{obs} is the measured data, Y^{sim} is the model simulation output, Y_0^{mean} *and* Y_s^{mean} *is* the observed data and simulated data for river flow, *i* is the *ith* measured of simulated data and *n* is the total number of observations (Moriasi *et al.,* 2007).

Coefficient of determination (R^2): Describes the degree of collinearity between the observed and simulated data. It is not recommended to use as a single criterion for evaluation of the model performance as it can give the same value for different magnitude data set.

$$R^2 = \quad R^2 = \frac{\sum_i [(Y^{obs} - Y_0^{mean})\,(Y^{sim} - Y_s^{mean})]^2}{\sum_i [(Y^{obs} - Y_0^{mean})^2 \sum_i [(Y^{sim} - Y_s^{mean})]^2} \cdots \textbf{(6)}$$

Where: Y^{obs} is the measured data, Y^{sim} is the model simulation output, Y_0^{mean} *and* Y_s^{mean} *is* the observed data and simulated data for river flow, *i* is the *ith* measured of simulated data and *n* is the total number of observations (Moriasi, et al., 2007).

RESULTS AND DISCUSSION

Hydrological model performance evaluation: The comparisons between the simulated and observed stream flow (Q) from ArcSWAT for the period 2002-2022 at the catchment outlet (Fig: 2) shows good accordance between the simulated and observed stream flow although some high flows and low flows are overestimated by the model. However, the simulated daily stream flow derived from the model matched well with the observed stream flow during calibration (R^2=0.85, NSE=0.82, KGE= 0.76, PBIAS

= -18.5) and validation (R^2=0.72, NSE=0.66, KGE= 0.66, PBIAS= -19.3) as shown by Table 2. The performance of ArcSWAT is considered to be acceptable for the stream flow calibration and validation at the catchment outlet as recommended by (Moriasi *et al.,*2007). The model performance for sediment yield is also good during calibration (R^2=0.80, NSE=0.81, PBIAS = -17) and validation (R^2=0.74, NSE=0.76, PBIAS= -19.7) as shown by Table 2.

Sensitivity analysis of LULC components that affect the hydrological response in River Ssezibwa basin: Ten sensitive parameters influencing hydrology and their ranking was done using SUFI-2 procedure in SWATCUP. The parameters were ranked in terms of their sensitivity to the SWAT model calibration (Table 3).

Global sensitivity Approach of the flow parameters was performed for calibration of the SWAT model using SWAT-CUP. The parameter that induced the most outputs is the most sensitive (Mosbahi, *et al.*, 2015). The Available Water capacity of the Soil Layer (Sol_AWC.sol), SCS runoff curve number (CN. Mgt), Average slope steepness (HRU_SLP.hru), Soil evaporation compensation factor (ESCO.hru) and Saturated hydraulic conductivity (SURLAG.bsn.) were the most sensitive respectively. The most sensitive parameter was the Available Water capacity of the Soil Layer (SOL.AWC.SOL). Generally, surface runoff parameters (Sol_AWC.sol, CN. Mgt, HRU_SLP.hru, ESCO.hru and SURLAG.bsn) are most sensitive to hydrological response in Upper Ssezibwa catchment.

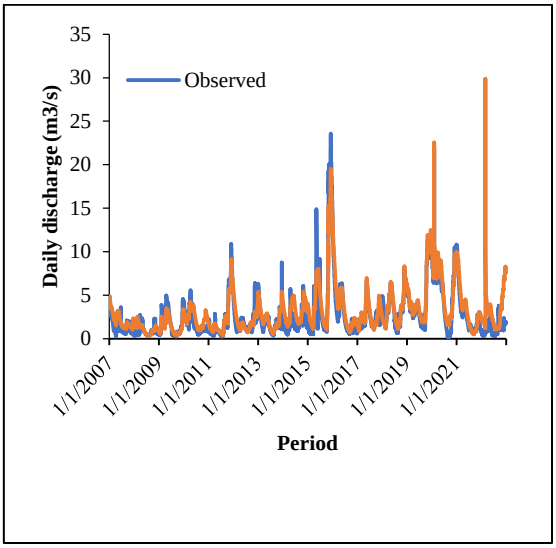

Fig 2: Observed and simulated discharge for the calibration (2007-2016) and validation (2017-2022) periods at the catchment outlet

Table 2: Model performance indicators for discharge and sediment yield at the catchment outlet

	Discharge							Sediment yield		
Simulation period (Daily)	**P-Factor**	**R-Factor**	**R^2**	**NSE**	**KGE**	**PBIAS**	**Mean Flow (simulated)**	**R^2**	**NSE**	**PBIAS**
Calibration (2007-2016)	0.62	0.38	0.9	0.82	0.76	-18.5	2.65(3.15)	0.8	0.81	-17
Validation (2017-2022)	0.59	0.45	0.7	0.65	0.66	-19.3		0.7	0.76	-19.7

Table 3: Ranking of the calibrated parameters, according to their sensitivity and significance

Rank	Parameter	Description	Final Range	Method
1	Sol_AWC.sol	Available water capacity of the soil layer	-0.12315	R
2	CN. mgt	SCS runoff curve number	-1.223492	R
3	HRU_SLP.hru	Average slope steepness	0.0 - 0.010634	V
4	ESCO.hru	Soil evaporation compensation factor	0.0 - 0.166683	V
5	SURLAG.bsn	Saturated hydraulic conductivity	0.060713 - 0.182883	V
6	GWQMN.gw	Threshold depth of water in the shallow aquifer required for return flow to occur	316.3638 - 428.2069	V
7	GW_DELAY.gw	Groundwater Delay	20.724407 - 62.389194	V
8	ALPHA_BF.gw	Base flow alpha factor (days)	0.383230 - 0.453092	V
9	SLSUBBSN.hru	Average slope length	11.305268- 21.171534	V
10	RCHRG_DP.gw	Deep aquifer percolation fraction	0.128689 - 0.192655	V

Note: "v" indicates a replacement method of the initial parameter value with the given value in the final range. "R" means a relative change to the initial parameter value.

Trend in historical and projected temperature and precipitation within the catchment: The influence of variation in rainfall and temperature on hydrology and sediment yield is simulated under Representative Concentration Pathways (RCP) 4.5 and 8.5. The projected (2025-2055) mean monthly temperature for both climate scenarios show a significant deviation from the historical (1981-2010), with high emission

scenarios (RCP 8.5) highly projecting increased monthly temperatures than medium emission scenarios (RCP 4.5) from the historical (Fig. 2). This indicates that RCP 8.5 is warmer than RCP 4.5 emission scenarios which is in agreement with the prediction range by IPCC (2014). However, the projections in mean monthly temperature follow the historical trends with lower temperatures observed during the dry season of June and July. Habtamu and Abete (2022) in a study on the effects of climate change on streamflow in Gelana watershed, Ethiopia found similar results that temperature increase will be higher under RCP 8.5 than RCP 4.5. Habtamu and Abate (2022) further observed increasing warming trends in Gelena catchment under the two scenarios for the period 2031-2050, 2051-2070, 2071-2090. Similarly, Kuma *et al.* (2021) noted that temperatures are likely to become warmer from 2021 to 2050 under RCP 4.5 and RCP 8.5 scenarios than the present in Bilate catchment, southern Ethiopia. Demmisie *et al.,* (2018) predicted increases in mean annual temperatures in the range of 0.5 ^{0}C to 1.5 ^{0}C between 2050s and 2080s in Kulfor river catchment, Ethiopia due to climate change.

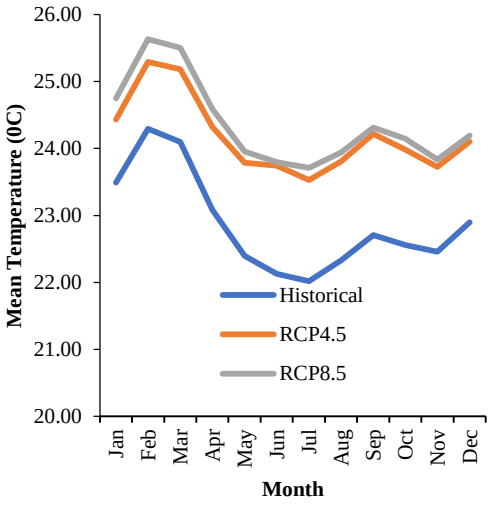

Fig 3: Comparison of mean Monthly temperatures between Historical (1981 - 2010) and the climate scenarios for the projected period of 2025 -2055

The climate scenarios project an increase in monthly precipitation with the highest observed in the long rain seasons of March – May. Generally, there is an increase in precipitation across the months except the months of June, September and October, which indicate a slight decline in projected precipitation (Fig 4). This indicates that flood risks are expected to be more severe in MAM than in JSO period. The increase in precipitation in Upper Ssezibwa catchment in the period 2025-2050 in comparison with 1980-2010 using model ensembles corresponds with the reported changes in annual precipitation in Lake Kyoga basin under the RCP 4.5 and RCP 8.5 by Nimusiima *et al.* (2019) and Nimusiima *et al*. (2014). Earlier studies by Seregina *et al.* (2019); Nicholson (2017) also projected increasing temperatures and precipitation in Horn of Africa and Eastern Africa respectively. In contrast however, Dibaba *et al.* (2020); Gadissa *et al.* (2019); Kuma *et al.,* (2021) projected decreasing trends of temperature and rainfall causing famine, drought and desertification.

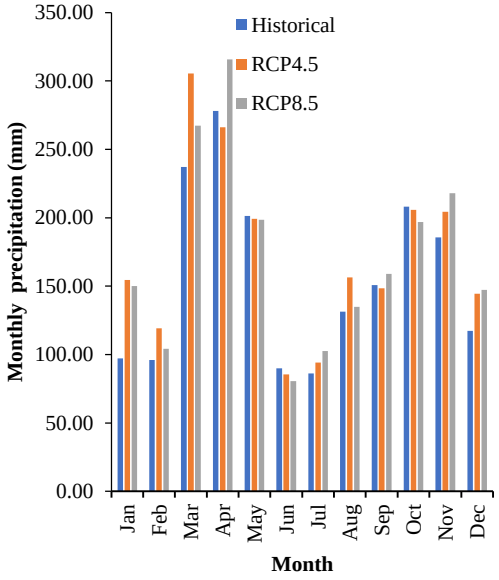

Fig 4: Comparison of mean monthly precipitation between Historical (1980 -2010) and the climate scenarios for the projected period of 2025 -2055

Projected changes in temperature and precipitation: Average annual temperature and precipitation projected by the model under the climate scenarios are presented in Table 4. An average temperature increment of 1.3^{o}C and 1.5^{o}C are projected by the assemble mean of the 29 GCMs under the two climate scenarios. Similarly, the relative change in precipitation is projected to increase by 10.9% and 10.4% under the RCP 4.5 and RCP 8.5 respectively from the historical period (1981-2010).

Table 4: Projected change in the annual temperature and precipitation

Parameter	RCP 4.5	RCP 8.5
ΔT (^{o}C)	1.3	1.5
Relative change in precipitation (%)	10.9	10.4

The ensemble mean of the 29 GCM model for the two climate scenarios exhibit an increase in monthly temperature with the highest being projected in the months of June and July of 1.61 ^{o}C and 1.69 ^{o}C under

RCP 4.5 and RCP 8.5, respectively (Fig 5). However, the monthly precipitation changes signals both a decrease and an increase for the future period for the ensemble mean model under the two climate scenarios (Fig 6) leading to high flow regimes and increased amounts of sediment yield as well as low flow regimes and low amounts of sediment yield during the low temperature scenarios. This will likely result into communities experiencing floods during the periods of high temperatures and water scarcity during the periods of low temperatures.

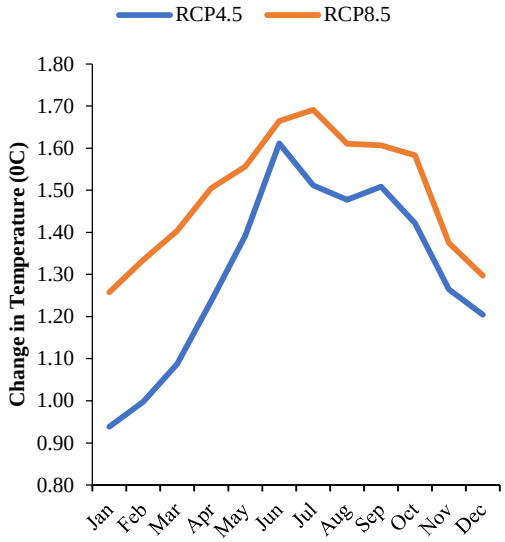

Fig 5: Projected change in mean monthly temperature

The ensemble mean indicates an increase in precipitation during most of the months of both wet and dry seasons under RCP 8.5 except for the months of May, June and October in which precipitation is projected to decrease. Likewise, for RCP 4.5, the ensemble mean projected a general increase in precipitation across the seasons of the year except for the month of April, May, June, September and October which show a decrease in projected precipitation ranging between -12% to -2.4%.

This is in conformity with Tigaba *et al.,* (2021) precipitation projection of an increase of 4.4% and a decrease by 0.7% in the period 2031-2060 and 2065-2094 respectively and temperature changes will vary between 1.3^{0}C to 2.7^{0}C and 2.0^{0}C and 3.8^{0}C in the period 2031-2060 and 2065-2094 for Gumera catchment, Ethiopia. Similar findings were reported by Gebremeskel and Kabede (2018) and Mengistu *et al.,* (2021) in studies carried in the Werii watershed of the Tekeze river basin, Northern Ethiopia and upper Blue Nile Basin of Ethiopia respectively. A study in South western Uganda projected increased changes in both rainfall and temperatures under RCP 4.5 and RCP 8.5 for the period 2040-60 (Bahati *et al.,* 2021). Contrary to the findings of the current study, Gadissa *et al.* (2019) projected a decline in rainfall by 7.97% and 2.53% and a temperature increase of 1.9 ^{0}C and 2.7^{0}C under RCP 4.5 and RCP 8.5 respectively in Central Rift Valley, Ethiopia.

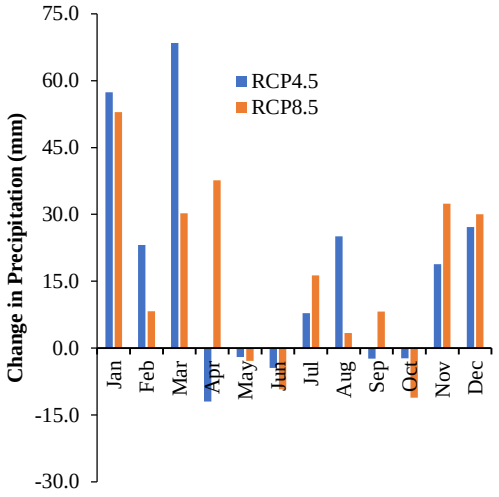

Fig 6: Projected changes in mean monthly precipitation and air temperature for the future period 2025-2055 in comparison with the historical period of 1981-2010.

Table 5: Projected changes in the selected water balance components simulated for the period 2025-2055 based on RCP4.5 and RCP8.5 scenarios.

Water balance components	Historical* (1981-2010)	RCP4.5 (2025 -2055)	RCP 8.5 (2025-2055)
Precipitation	1814	2022 (11.4%)	2013.8 (11.01%)
Surface runoff [mma-1]	1.01	3.7 (266.3%)	3.3 (226.7%)
Lateral flow [mma-1]	0.06	0.07 (16.7%)	0.07(16.7%)
Groundwater flow [mma-1]	473.9	567.7 (19.7%)	562.7 (18.7%)
Water yield [mma-1]	475	571.5 (20.3%)	566.2 (19.2%)
Deep aquifer recharge [mma-1]	90.7	109.4 (20.6%)	109.1(20.3%)
Actual Evapotranspiration [mma-1]	1248.3	1341.1 (7.4%)	1338.7 (7.2%)
Potential Evapotranspiration [mma-1]	1710.6	1774.7 (3.7%)	1783.9 (4.3%)
Percolation [mma-1]	564.7	675.5 (19.6%)	670.1 (18.7%)

Historical annual average precipitation is based on GCM simulations (1981-2010).

Projected changes in the Water Balance: The ensemble mean scenario projects a wetter future with 208 mm (RCP 4.5) and 200 mm (RCP 8.5) additional precipitation (Table 5). Changes in the selected water balance components indicate an increase in the future for both the climate scenarios.

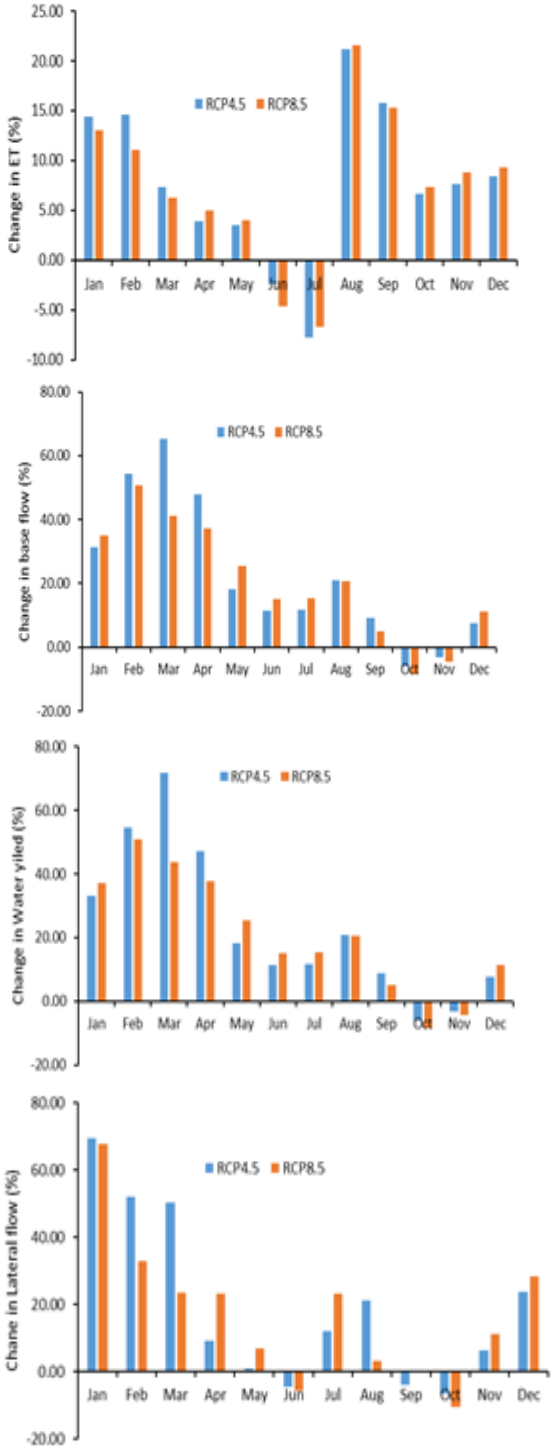

Fig 7: Projected monthly changes (%) in water budget components from under the climate scenarios for period 2025-2055

However, the projected increase is higher for surface runoff (i.e. 266% and 226% for RCP 4.5 and RCP 8.5, respectively), followed by percolation, groundwater/base flow, water yield (summation of surface runoff, lateral flow and groundwater flow/base flow) and deep aquifer recharge which are projected to increase beyond 18% from the historical state. The increases in the stream flow components of surface runoff, lateral flow, ground water recharge provide impetus for possible flooding in Upper Ssezibwa catchment and the associated problems such as loss of life, destruction of property and emergence and spread of water borne diseases like cholera. Figure 7 depicts the intra-annual variability in mean monthly actual evapotranspiration (ET), base flow, water yield, and lateral flow projected by the RCM ensemble mean for the two RCP scenarios

Projected changes in base flow indicate the dry and wet seasons to experience an increment except for the month of October and November in which there is projected decrease in the base flow within the catchment. Increment in baseflow is an indicator of ground water availability during the dry seasons implying that river Ssezibwa flows will be maintained. Likewise, a similar trend is projected for water yield and lateral flow hydrological processes in the catchment. A study by Habtamu and Abate (2022) in Gelana watershed Ethiopia projected that as a result of variation in climate, the mean annual surface runoff, ground water and total water yield will decrease yet actual evapotranspiration is expected to increase in all feature periods in the watershed under RCP 4.5 and RCP 8.5 contrary to the findings of the current study. Equally, Dibaba *et al.,* (2020) found a decline in surface runoff, ground water and total water yield in Finchaa watershed, Ethiopia as a result of increasing temperatures amplified by the increases in evapotranspiration.

Accordingly, actual evapotranspiration is projected to increase for the wet seasons and the dry periods of DJF with the months of June and July indicating a decline in ET under the two climate scenarios. The highest increase in ET is projected in the month of August.

Projected changes in discharge and sediment yield: Table 6 shows the projected changes in annual sediment yield and discharge simulated by the RCM ensemble mean for the two RCP climate scenarios. Accordingly, a significant increase in sediment yield (56.7%) within the catchment in the future is projected for both the climate scenarios. Conversely, annual discharge is also projected to increase within the catchment due to the impacts of climate change,

with RCP 4.5 causing more discharge (18.4%) than RCP 8.5 (16.3%) from the historical period. The increase in sediment yield and discharge possess challenges of increased siltation of the river channel, flooding and affecting the water quality leading to destruction of property, loss of lives and spread of waterborne diseases. In contrast with the current results, a study by Gadissa *et al.,* (2019) discovered that due to variations in climate, streamflow was reduced by 25.1% when precipitation decreased by 10% and by 15.1% when evapotranspiration increased by 10%

Table 6: Projected changes in the annual sediment yield and discharge simulated for the period 2025-2055 based on RCP4.5 and RCP8.5 scenarios.

Components	Historical (1981-2010)	RCP4.5 (2025 -2055)	RCP 8.5 (2025-2055)
Precipitation	1814	2022 (11.4%)	2013.8 (11.01%)
Sediment yield (t/ha)	0.003	0.02 (56.7%)	0.02(56.7%)
Discharge (m3/s)	4.85	5.8 (18.4%)	5.7 (16.3%)

Table 7: Projected changes in the mean monthly sediment yield and discharge simulated for the period 2025-2055 based on RCP4.5 and RCP8.5 scenarios.

Month	% change			
	Surface runoff		Sediment yield	
	RCP 4.5	RCP 8.5	RCP 4.5	RCP 8.5
January	6713.8	8784.4	13090.4	16766.5
February	3018.6	50.5	4993.2	104.6
March	465.7	198.4	525.4	225.1
April	-27.2	133.5	-6.1	132
May	110.3	-4.1	198.5	-26.9
June	0	0	0	0
July	0	0	0	0
August	0	0	0	0
September	-46.5	30.9	42.8	275.2
October	-26.4	-44	-35.4	-56.7
November	94.2	236.6	391.5	810.2
December	433.5	720.1	615.4	1578.8

Fig 8 presents the intra-annual variability in mean monthly discharge projected by the RCM ensemble mean for the two RCP scenarios. The mean monthly discharge will be seasonally affected by the changes in precipitation. In fact, there is a distinct difference between the long rain wet seasons (MAM) and dry (JJA) season. More discharge is projected in the long rains (MAM) and in the short rains, discharge will increase except for the month of October which indicates a decrease. As expected, low discharge will be pronounced during the dry seasons and higher discharge will occur in the long rains (with an increase of 15% to 55%) for both RCP scenarios, although the changes are more pronounced under RCP4.5. Furthermore, sediment yield is projected to increase across the seasons except in some wet months of October (-35% and -56.7% for RCP 4.5 and RCP 8.5, respectively), April (a decline of -6.1% under RCP 4.5) and May (-26.9% under RCP 8.5).

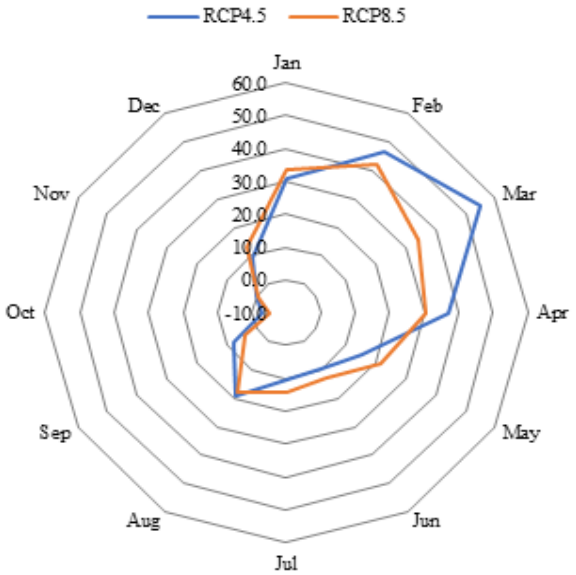

Fig 8: Projected change in monthly discharge for the period 2025-2055 under the climate scenarios

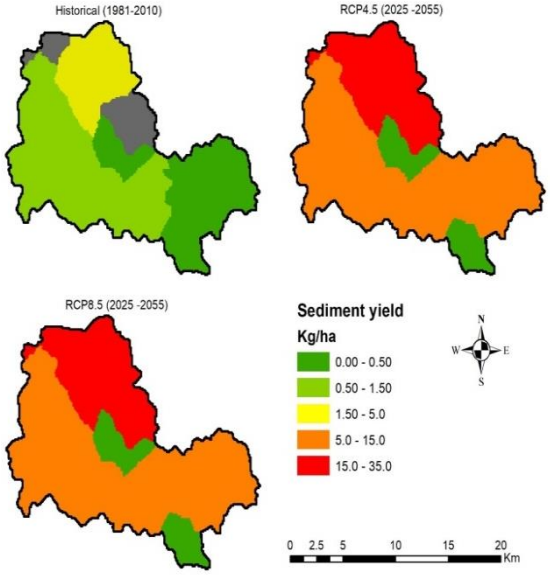

Fig 9: Comparison of sediment yield hotspots for the historical (1981-2010) and projected period (2025-2055) in Ssezibwa catchment

The highest projected increase (i.e. 49 -168 times higher than the historical sediment yield) is expected to occur in the months of January and February (Table 7). Similar trends are observed for surface runoff within the catchment (Table 7). Fig 9 depicts the projected impacts of climate variability on the spatial distribution of sediment yield within the catchment. Results indicate that climate variability will have a significant impact on sediment yield

across the catchment with hotspots mainly observed at the upper slopes of the catchment than the middle and lower parts for the two climate scenarios. This is in harmony with Ranjan and Mishra (2023) discovery that because of climate change, streamflow and sediment yield are likely to increase by 6.38% (6.06) and 4.43% (7.89%) in 2020-2046 and by 29.78% (36.90) and 37% (46.43%) in 2047-2073 respectively in Mahanadi River Basin, India.

Conclusion: The study projected an increase in the variation of temperature, precipitation and water balance components between 2025-2055 under RCP 4.5 and RCP 8.5. Projections indicate a likely increase in surface runoff, lateral flow, ground water flow and water yield indicating sufficient water availability in the catchment in the future which can be utilized in agriculture and other economic activities. An increase in surface runoff indicates high flows which are likely to result in flood risks, natural disasters and emergence of waterborne diseases in the future. Sediment yield is projected to increase in the two emission scenarios indicating that the catchment is a likely recipe for the deposition of the sediment on the flood plain and river channels. Therefore, government and physical planners need to design appropriate interventions to prevent natural disasters as well as to mitigate the problems arising from floods in the catchment.

Declaration of conflict of interest: The authors declare no conflict of interest.

Data Availability Statement: All data generated and analyzed during this study are included in this published article.

REFERENCES

Abd El-Hamid, HT; Caiyong, W., Hafiz, MA; Mustafa, EK (2020). Effects of land use/land cover and climatic change on the ecosystem of North Ningxia, China. *Arab J Geosci* 13, 1099. DOI: https://doi.org/10.1007/s12517-020-06047-6

Abbaspour, KC (2015). SWAT- Cup: SWAT Calibration and uncertainty program-A User manual. EAWAG.

Ampurire, P (2018). Police rescues 18 people trapped on island due to flooded River Ssezibwa. *Soft Power*.

Arnold, JG; Moriasi, DN; Gassman, PW; Abbaspour, KC; White, MJ; Srinivasan, R; Santhi, C; Harmel, RD; van Griensven, A; van Liew, MW; Kannan, N; Jha, MK (2012). SWAT: Model use, calibration, and validation. *Transactions Of The Asabe* 55(4): 1491-1508. DOI: https://doi.org/10.13031/2013.42256

Azari, M; Moradi, HR; Saghafian, B; Faramarzi, M (2016) Climate change impacts on streamflow and sediment yield in the North of Iran. *Hydrological Sciences Journal,* 61:1, 123-133, DOI: https://doi.org/10.1080/02626667.2014.967695

Bahati, HK; Ogenrwoth, A; Sempewo, JI (2021). Quantifying the potential impacts of land-use and climate change on hydropower reliability of Muzizi hydropower plant, Uganda. *J. Water Clim. Change.* DOI: https://doi.org/10.2166/wcc.2021.273

Banda, VD; Dzwairo, RB; Singh, SK; Kanyerere, T (2022). Hydrological Modelling and Climate Adaptation under Changing Climate: A Review with a Focus in Sub-Saharan Africa. *Water*, 14, 4031. DOI: https://doi.org/10.3390/w14244031

Bhatta, B; Shrestha, S; Shrestha, PK.; Talchabhadel, R (2019). Evaluation and application of a SWAT model to assess the climate change impact on the hydrology of the Himalayan River Basin. *Catena*, 181, 104082. DOI: https://doi.org/10.1016/j.catena.2019.104082

Cibin, R; Sudheer, KP; Chaubey, I (2010). Sensitivity and identifiability of stream flow generation parameters of the SWAT model. *Hydrological Processes*, 24 (9), 1133–1148. DOI: https://doi.org/10.1016/j.rsase.2019.01.00310.1002/hyp.v24:9

Dai, C; Qin, XS; Lu, WT; Huang, Y (2020). Assessing adaptation measures on agricultural water productivity under climate change: a case study of Huai River Basin, China. *Sci. Total Environ*. 721, 137777. DOI: https://doi.org/10.1016/j.scitotenv.2020.137777

Demmissie, NG; Demissie, TA; Tufa, FG (2018). Predicting the impact of climate change on Kulfo river flow. *Hydrology* 6 (3), 78. DOI: https://doi.org/10.11648/j.hyd.20180603.11.

Dibaba, WT; Demissie, TA; Miegel, K (2020) Watershed hydrological response to combined land use/land cover and climate change in highland Ethiopia: Finchaa catchment. *Water* (Switzerland) 12 (6).

dos Santos, JYG; Montenegro, SMGL; da Silva, RM; Santos, CAG; Quinn, NW; Dantas, APX; Neto, AR (2021). Modeling the impacts of future LULC and climate change on runoff and sediment yield in a strategic basin in the Caatinga/Atlantic Forest ecotone of Brazil. *Catena* 203, 105308

Dou, X; Ma, X; Zhao, C; Li, J; Yan, Y; Zhu, J (2022). Risk assessment of soil erosion in Central Asia under global warming. *Catena*. DOI: https://doi.org/10.1016/j.catena.2022.106056

Engida, TG; Nigussie, TA; Aneseyee, AB; Barnabas, J (2021). Land Use/Land Cover Change Impact on Hydrological Process in the upper Baro Basin, Ethiopia. *Appl. Environ. Soil Sci.* DOI: https://doi.org/10.1155/2021/6617541

Gadissa, T; Nyadawa, M; Mutua, B; Behulu, F (2019). Comparative assessment of the effect of climate change and human activities on streamflow regimes in Central Rift Valley Basin, Ethiopia. *Am. J. Wat. Resour.* 7 (1), 23–29. DOI: https://doi.org/10.12691/ajwr-7-1-4

Gebremeskel, G; Kebede, A (2018). Estimating the effect of climate change on water resources: integrated use of climate and hydrological models in the Werii watershed of the Tekeze river basin, Northern Ethiopia. *Agric. Nat. Resour.* 52 (2), 195–207. DOI: https://doi.org/10.1016/j.anres.2018.06.010

Getahun, YS; van Lanen, H (2015). "Assessing the impacts of land use-cover change on hydrology of Melka Kuntrie subbasin in Ethiopia, using a conceptual hydrological model". *Hydrology: Current Research*, 6(3), 1–11. DOI: https://doi.org/10.4172/2157-7587.1000210

Gupta, HV; Kling, H; Yilmaz, KK; Martinez, GF (2009). Decomposition of the mean squared error and NSE performance criteria: Implications for improving hydrological modelling. *J. Hydrol.*, 377(1-2), 80–91.DOI: https://doi.org/10.1016/j.jhydrol.2009.08.003

Habtamu, D; Abate, B (2022). Effect of climate change on streamflow in the Gelana watershed, Rift valley basin, Ethiopia. *J. Wat. Climate Change.* 13(5): 2205 DOI: https://doi.org/10.2166/wcc.2022.059

Hirschberg, J; Fatichi, S; Bennett, GL; McArdell, BW; Peleg, N; Lane, SN; Schlunegger, F; Molnar, P (2021). Climate change impacts on sediment yield and debris flow activity in an Alpine catchment. *J. Geophysic. Res. Earth Surface.* 126, e2020JF005739. DOI: https://doi.org/10.1029/2020JF005739

Kandissounon, GA; Kalra, A; Ahmad, S (2018) Integrating system dynamics and remote sensing to estimate future water usage and average surface runoff in Lagos, Nigeria. *Civil Engineer. J.* 4(2), 378-393. DOI: https://doi.org/10.28991/cej-030998

Karvonen, T; Koivusalo, H; Jauhiainen, M; Palko, J; Weppling, K (1999). A hydrological model for predicting runoff from different land use areas. *J. Hydrol.* 217(3-4): 253–265. DOI: https://doi.org/10.1016/S0022-1694(98)00280-7

Kimbowa, I (2019). Transport Paralysed As River Sezibwa Floods. *Uganda Radio Network.*

Kuma, HG; Feyessa, FF; Demissie, TA (2021). Hydrologic responses to climate and land-use/land-cover changes in the Bilate catchment, Southern Ethiopia. *J. Wat. Climate Chang.* 12 (8), 3750–3769. DOI: https://doi.org/10.2166/wcc.2021.281

Lu, XX; Ran, LS; Liu, S; Jiang, T; Zhanga, HR; Wang JJ (2013). Sediment loads response to climate change: A preliminary study of eight large Chinese rivers. *Intern. J. Sediment Res.* 28 (1), 1-14.

Mengistu, D; Bewket, W; Dosio, A; Panitz, HJ (2021). Climate change impacts on water resources in the Upper Blue Nile (Abay) River Basin, Ethiopia. *J. Hydrol.* 592. DOI: https://doi.org/10.1016/j.jhydrol.2020.125614

Moriasi, D; Arnold, J; van Liew, M; Bingner, R; Harmel, R; Veith, T (2007). Model evaluation guidelines for systematic quantification of accuracy in watershed simulations. *Trans. ASABE*, 50(3), 885-900. DOI: https://doi.org/10.13031/2013.23153

Mosbahi, M; Benabdallah, S; Boussema, MR (2015). Sensitivity analysis of a GIS-based model: A case study of a large semi-arid catchment. *Earth Sci Inform* 8: 569–581. DOI: https://doi.org/10.1007/s12145-014-0176-0

Muzaale, F (2007). Uganda: R. Ssezibwa Floods Sink 65 Homes in Mukono, Kayunga. *The Daily Monitor*, September, 19, 2007.

Muzaale, F (2019). One dead as floods damage bridge on River Ssezibwa. *The Daily Monitor*, November, 5, 2019.

Nasasira, D (2021). PM Nabbanja delivers relief items to flood victims in Kayunga District. Office of the Prime Minister.

NEMA (2016). State of the Environment Report for Uganda 2014. National Environment Management Authority (NEMA), Kampala.

Nicholson, SE (2017). Climate and climate variability of rainfall over eastern Africa. *Rev. Geophys*., 55, 590–635. DOI: https://doi.org/10.1002/2016RG000544

Nimusiima, A; Basalirwa, CPK; Majaliwa, JGM; Mbogga, SM; Mwavu, EN; Namaalwa, J; Okello-Onen, J (2014). Analysis of Future Climate Scenarios over Central Uganda Cattle Corridor. *J. Earth Sci. Clim. Chang*. 5, 10. DOI: https://doi.org/10.4172/2157-7617.1000237

Nimusiima, A; Kisembe, J; Nakyembe, N (2019). Evaluation of past and future extreme rainfall characteristics over Eastern Uganda. *J. Environ. Agric. Sci*. 18, 38–49.

Ochola, GO; Nyamai, DO; Okeyo-Owuor JB (2019). Impacts of Land Use and Land Cover Changes on the Environment associated with the Establishment of Rongo University in Rongo Sub-County, Migori County, Kenya. *Int J Environ. Sci Nat Res*. 21(5): 556072. DOI: https://doi.org/10.19080/IJESNR.2019.21.556072

Perron, JT (2017). Climate and the pace of erosional landscape evolution. *Ann. Rev. Earth. Planet. Sci.* 45(1), 561–591.

Ranjan, R; Mishra, A (2023). Climate change impact on streamflow and suspended sediment load in the flood-prone river basin. *Journal of Water and Climate Change*, 14 (7) 2260. DOI: https://doi.org/10.2166/wcc.2023.037

Seregina, LS; Fink, AH; van der Linden, R; Elagib, NA; Pinto, JG (2019). A new and flexible rainy season definition: Validation for Greater Horn of Africa and application to rainfall trends. *Int. J. Climatol*. 39, 989–1012. DOI: https://doi.org/10.1002/joc.5856

Sok, T; Ich, I; Tes, D; Chan, R; Try, S; Song, L; Ket, P; Khem, S; Oeurng, C (2022). Change in Hydrological Regimes and Extremes from the Impact of Climate Change in the Largest Tributary of the Tonle Sap Lake Basin. *Water*, 14(9), 1426. DOI: https://doi.org/10.3390/w14091426

Tamm, O; Maasikamäe, S; Padari, A; Tamm, T (2018). Modelling the effects of land use and climate change on the water resources in the eastern Baltic Sea region using the SWAT model. *Catena*, 167, 78–89. DOI: https://doi.org/10.1016/j.catena.2018.04.029

Thackeray, CW; Hall, A; Norris, J; Chen, D (2022). Constraining the increased frequency of global precipitation extremes under warming. *Nat. Clim. Chang.*: **2**, 441–448. DOI: https://doi.org/10.1038/s41558-022-01329-1

The Independent (2020). Kayunga leaders seek help to rescue residents in flooded areas. Authors, June 22, 2020

.